The EMBO Journal Vol.17 No.15 pp.4213–4225, 1998

Impaired cerebral cortex development and blood pressure regulation in FGF-2-deficient mice

Rosanna Dono[1], Gemma Texido, Rudolf Dussel[2], Heimo Ehmke[1,2] and Rolf Zeller[1]

EMBL, Meyerhofstrasse 1, D-69117 Heidelberg and [2]Institute of Physiology, University of Heidelberg, Im Neuenheimer Feld 326, D-69120 Heidelberg, Germany

[1]Corresponding authors

Fibroblast growth factor-2 (FGF-2) has been implicated in various signaling processes which control embryonic growth and differentiation, adult physiology and pathology. To analyze the *in vivo* functions of this signaling molecule, the FGF-2 gene was inactivated by homologous recombination in mouse embryonic stem cells. FGF-2-deficient mice are viable, but display cerebral cortex defects at birth. Bromodeoxyuridine pulse labeling of embryos showed that proliferation of neuronal progenitors is normal, whereas a fraction of them fail to colonize their target layers in the cerebral cortex. A corresponding reduction in parvalbumin-positive neurons is observed in adult cortical layers. Neuronal defects are not limited to the cerebral cortex, as ectopic parvalbumin-positive neurons are present in the hippocampal commissure and neuronal deficiencies are observed in the cervical spinal cord. Physiological studies showed that FGF-2-deficient adult mice are hypotensive. They respond normally to angiotensin II-induced hypertension, whereas neural regulation of blood pressure by the baroreceptor reflex is impaired. The present genetic study establishes that FGF-2 participates in controlling fates, migration and differentiation of neuronal cells, whereas it is not essential for their proliferation. The observed autonomic dysfunction in FGF-2-deficient adult mice uncovers more general roles in neural development and function.

Keywords: autonomic dysfunction/blood pressure/cerebral cortex/FGF-2/neural development

Introduction

Members of the fibroblast growth factor (FGF) family and their high affinity tyrosine kinase FGF receptors (FGFR) have been implicated in embryonic growth and patterning and, in particular, during central nervous system (CNS) development (reviewed by Eckenstein, 1994). Studies using *Xenopus laevis* embryos revealed roles for FGF signaling during establishment of initial posterior neural tube identities (reviewed by Sasai and De Robertis, 1997). Similarly, FGFR1-deficient mouse embryos display neural tube defects, which most likely arise from incorrect specification of neuroectodermal cell fates (Yamaguchi *et al*., 1994). During initial patterning of the brain vesicle, FGF-8 is expressed by the isthmus, the organizer which separates mid- from hindbrain (Crossley *et al*., 1996). Ectopic rostral FGF-8 application or expression results in transformation of fore- into midbrain structures, indicating that FGF-8 determines midbrain identity (Crossley *et al*., 1996; Lee *et al*., 1997). The spatial distribution of FGF-3 in the developing hindbrain is consistent with roles in establishment of rhombomere boundaries (Wilkinson *et al*., 1988), but no changes in rhombomere identities are observed in FGF-3-deficient embryos (Mansour *et al*., 1993).

Roles for FGF-2 during CNS morphogenesis have been postulated as high levels are detected from neurulation onwards (Dono and Zeller, 1994; Riese *et al*., 1995; reviewed by Eckenstein, 1994). Furthermore, overexpression of specific FGF-2 isoforms in the neural tube of transgenic mouse embryos provided evidence for growth-regulatory functions during spinal cord morphogenesis (Zuniga Mejia Borja *et al*., 1996). Such a proposed mitogenic role in neurogenesis was also supported by studies using cultured neural progenitors. These studies indicated that FGF-2 levels regulate proliferation of specific neural cell types (reviewed by Vescovi *et al*., 1993; Temple and Qian, 1995). In contrast, other studies provided evidence that FGF-2 participates in promoting differentiation and long-term survival of neurons in culture. These *in vitro* studies suggested that FGF-2 functions in a concentration-dependent manner to regulate mainly proliferation, but also differentiation and survival of neural progenitors (Petroski *et al*., 1991; Ray *et al*., 1993; Ghosh and Greenberg, 1995; Vicario-Abejon *et al*., 1995; Qian *et al*., 1997).

In addition to the CNS, FGF-2 is expressed during other developmental processes such as limb, kidney and cardiovascular morphogenesis (e.g. Dono and Zeller, 1994). Of particular interest for the present study is expression by vascular smooth muscle cells, endothelial cells and post-mitotic cardiomyocytes (Kardami and Fandrich, 1989; Lindner and Reidy, 1993; Cuevas *et al*., 1996). Both acute (Cuevas *et al*., 1991) and chronic (Lazarous *et al*., 1995) intravenous infusion of recombinant FGF-2 in normotensive animals induces a significant reduction in blood pressure (hypotension), which is mediated partly by release of nitric oxide and activation of ATP-sensitive K^+ channels (Cuevas *et al*., 1991). In the spontaneously hypertensive rat, endogenous levels of FGF-2 in endothelial cells are chronically reduced and blood pressure can be lowered by chronic infusion of FGF-2 (Cuevas *et al*., 1996). These studies suggested that FGF-2 functions in an antihypertensive vasodilator cascade. In contrast, other studies indicated that FGF-2 acts as a potent mitogen for smooth muscle cells *in vitro* and regulates blood vessel growth *in vivo* (Lazarous *et al*., 1995; Davis *et al*., 1997). Furthermore, FGF-2 is released

from cardiomyocytes upon increased mechanical load (Clarke *et al*., 1995) and induces adaptive myocardial growth (Kaye *et al*., 1996). These studies suggested that FGF-2 signaling functions in the cardiovascular adaptations leading to a chronic blood pressure increase (hypertension).

To study the essential *in vivo* functions of FGF-2 during embryogenesis and in adult physiology, the FGF-2 gene was inactivated in mice using homologous recombination in embryonic stem (ES) cells. FGF-2-deficient mice show neuronal defects in the cerebral cortex, hippocampal commissure and spinal cord. In particular, a fraction of neuronal precursors fail to colonize their normal target layers II and III during cerebral cortex development. Furthermore, adult FGF-2-deficient mice have a reduced blood pressure. Continued angiotensin II infusion induced hypertension of a similar magnitude as in wild-type litter mates, demonstrating an intact responsiveness of their cardiovascular system. In contrast, infusion of isoproterenol into FGF-2-deficient mice uncovered an impairment of their baroreceptor reflex. Therefore, blood pressure regulation is affected by an autonomic dysfunction.

Results

Mice homozygous for a loss-of-function FGF-2 allele are viable and fertile

The first coding exon (e1, Figure 1A) of the murine FGF-2 gene encodes three protein isoforms (Figure 1D), which are translated by alternative initiation. Therefore, the complete first FGF-2 coding exon and parts of the 5′- and 3′-flanking intronic sequences were replaced by the neomycin resistance gene (neo, Figure 1A) in the opposite transcriptional orientation using homologous recombination in ES cells. Chimeric mice were generated from correctly targeted ES cells and crossed to C57BL/6J mice for germline transmission. Subsequently, homozygous FGF-2$^{-/-}$ mice were obtained in a mixed C57BL/6J×129/Sv genetic background. Genotyping of their offspring at birth and weaning age (Figure 1B and C) showed that FGF-2$^{-/-}$ mice are born alive, mature normally to adulthood and are fertile (data not shown). As FGF-2 is expressed from gastrulation onwards (Riese *et al*., 1995), it was essential to determine that a complete loss-of-function FGF-2 allele had been generated. Normalized amounts of proteins from brains of newborn mice (Figure 1D) and embryos (data not shown) of all three genotypes were analyzed using specific FGF-2 antibodies (Dono and Zeller, 1994). Western blot analysis showed that levels of all three FGF-2 isoforms are reduced to about half in heterozygous mice (Figure 1D, compare lane 10 with 9), whereas no FGF-2 proteins are detected in homozygous litter mates (Figure 1D, lanes 11 and 12, see also Figure 2B). Further analysis confirmed that no truncated proteins are expressed and that there is no embryonic rescue by maternal FGF-2 protein (data not shown). In summary, expression of all three FGF-2 isoforms is abolished and a complete loss-of-function allele has been generated.

Development of the cerebral cortex is impaired in FGF-2-deficient mice

FGF-2 is expressed in the CNS from its earliest developmental stages onwards. In the forebrain, FGF-2 proteins are first detected during embryonic day 9.5 (Nurcombe *et al*., 1993). Figure 2 shows the distribution of FGF-2 proteins (Figure 2A–D) and transcripts of their high affinity FGF receptor isoforms [FGFR1-IIIc (Figure 2E) and FGFR2-IIIc (Figure 2F); reviewed by Miller and Rizzino (1994)] during embryonic days 14.5 and 16, respectively. At this developmental stage, the highest levels of FGF-2 proteins are present in the cerebral hemispheres, whereas levels are lower in more caudal brain regions and in the spinal cord (Figure 2A). As expected from molecular analysis (Figure 1D), no FGF-2 proteins are detected in FGF-2-deficient embryos (Figure 2B). In cerebral hemispheres, FGF-2 protein levels are highest in the ventricular and sub-ventricular zones of the lateral ventricles (Figure 2C and D), the region where neural progenitors are born and determined (Bayer and Altman, 1991). In contrast, cells within the cortical plate express much lower amounts of FGF-2 (Figure 2D). Similarly, transcripts encoding FGFR1-IIIc (Figure 2E) and FGFR2-IIIc (Figure 2F) isoforms are co-expressed in both ventricular and sub-ventricular zones. FGFR2-IIIc isoform transcripts persist in the cortical plate, whereas FGFR1-IIIc expression is much lower (compare Figure 2F with E). No changes in FGFR transcripts were observed in brains of FGF-2-deficient embryos (data not shown).

To determine whether FGF-2 is necessary for embryonic CNS morphogenesis, brains of wild-type and FGF-2-deficient newborn litter mates were analyzed by comparative histology (Figure 3). Serial coronal sections of FGF-2-deficient mice showed no gross morphological abnormalities (compare Figure 3A with B and C). In newborn mice, differentiation of the cerebral cortex progresses from deep to superficial layers (VI–I, see Figure 3D; Bayer and Altman, 1991) and large pyramidal neurons are apparent (Figure 3D and G). No differences were observed between wild-type (+/+) and heterozygous (+/–) mice (data not shown). However, FGF-2-deficient litter mates display defects in organization and differentiation of their cerebral cortex. In particular, the thickness of the cerebral cortex in homozygous (–/–) mice is reduced by ~10% in comparison with their control litter mates at birth (+/+; +/–, Table IA and B; $P < 0.05$). At the cellular level, all differentiating cortical layers appear compressed and less distinct (compare Figure 3D with E and F). Differentiated, large pyramidal neurons are apparent in newborn wild-type mice (Figure 3D and G), whereas only a few are observed in FGF-2-deficient litter mates (Figure 3E and F, and H and I). This phenotype reveals a requirement for FGF-2 for embryonic cerebral cortex morphogenesis.

Neuronal cell migration is affected during cerebral cortex development in FGF-2-deficient mice

Early patterning and development of the embryonic brain appear normal in FGF-2-deficient embryos, as neither spatial nor temporal changes were detected in molecular markers during embryonic days 11–16 (*BF1*, *Emx1*, *Otx1*, *Otx2*, *mtll*; data not shown). After compartmentalization of the brain vesicle, the neurons of the cerebral cortex are generated by the pseudo-stratified ventricular epithelium that lines the lateral ventricles in the telencephalon. Cortical neurogenesis is marked by the appearance of the first post-mitotic neurons during embryonic day 11 and

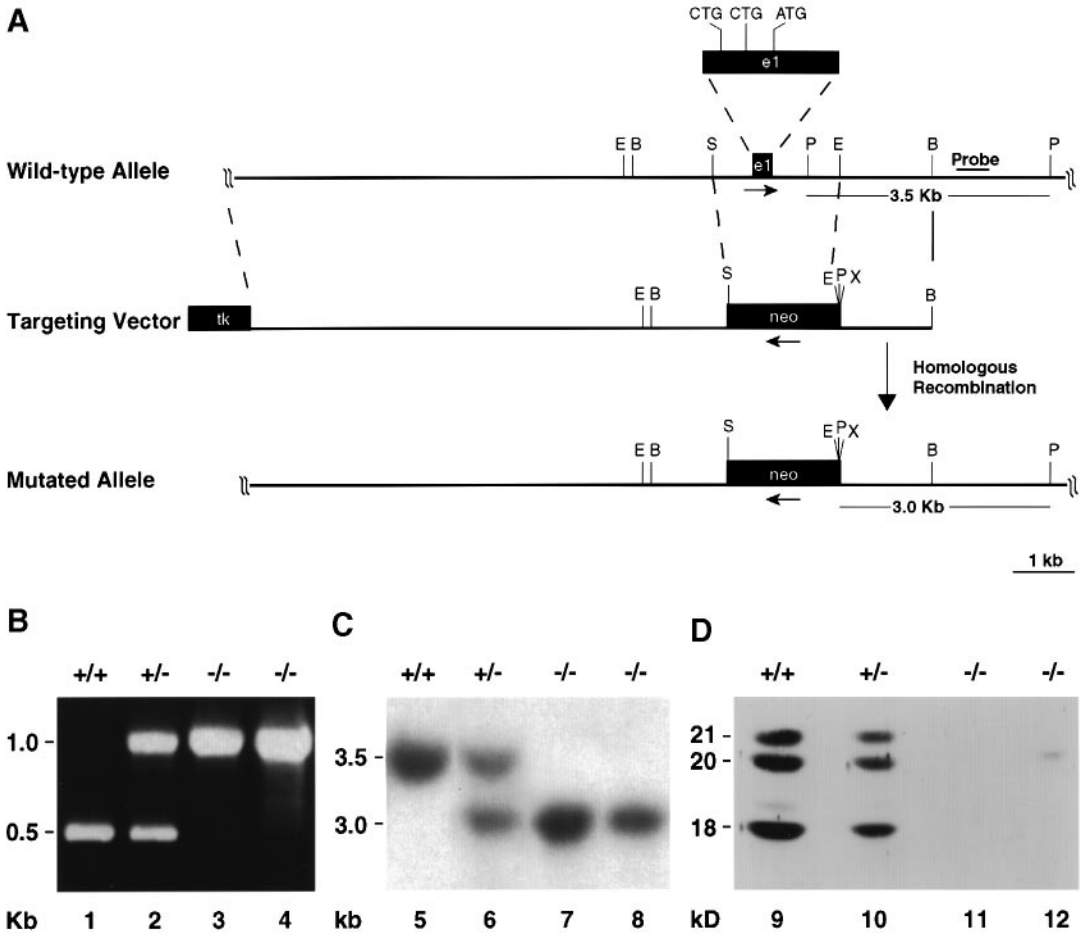

Fig. 1. Generation of a loss-of-function FGF-2 allele by gene targeting. (**A**) Using homologous recombination in ES cells, the first coding exon (e1) of FGF-2 and flanking intronic sequences were replaced by the PGK-neo cassette in the opposite transcriptional orientation (arrows indicate transcriptional orientation). Three FGF-2 protein isoforms normally are synthesized by alternative translation from an ATG and two upstream in-frame CTG start codons (see D). Probe: a DNA fragment located 3′ to the short arm is used to discriminate the wild-type and mutated alleles by Southern blotting (see C). E. *Eco*RI; B, *Bam*HI; S, *Sal*I; P: *Pst*I; X, *Xba*I. (**B**) PCR analysis of genomic DNA using specific oligos. A 0.5 kb PCR fragment is derived from intronic sequences of the wild-type allele, whereas a 1 kb fragment is amplified from the recombined allele with the neo cassette. (**C**) Southern blot analysis of genomic DNA to detect correct 3′ recombination (using the probe shown in A). A 3.5 kb *Pst*I fragment marks the wild-type allele, whereas a 3 kb *Pst*I fragment indicates the disrupted locus (see A). (**D**) Immunoblot analysis of protein extracts prepared from brains of newborn mice. All extracts were checked for integrity and normalized for total protein content. Affinity-purified polyclonal FGF-2 antibodies were used to detect the murine FGF-2 proteins. Two larger Leu-initiated isoforms (21 and 20 kDa) are synthesized in addition to the Met isoform (18 kDa) in wild-type mice (lane 9). Note that protein levels are halved in heterozygous mice (lane 10), whereas no FGF-2 proteins are detected in homozygous mice (lanes 11 and 12). The weak band in lane 12 is not detected reproducibly and is of a size (~20.5 kDa) different from any of the three FGF-2 isoforms.

continues until embryonic day 17. Determined neurons leave the ventricular zone through the intermediate zone and migrate outwards along radial glial tracts. In the cortical plate, they colonize their respective target layers that form successively from deep to superficial (layer VI–II) as cortical development proceeds. After completing migration, cortical neurons undergo terminal differentiation which continues after birth (reviewed by Bayer and Altman, 1991; Hatten, 1993).

To determine whether proliferation of cortical progenitors is affected in FGF-2-deficient embryos, nuclei of proliferating cells were pulse-labeled for 1 h with 5-bromodeoxyuridine (BrdU). Quantitative analysis (Table IC) shows that proliferation of progenitor cells within the ventricular zone of FGF-2-deficient embryos (Figure 4B) is indistinguishable from that of wild-type litter mates (Figure 4A) during embryonic days 14.5–15. Analysis of brains from embryonic days 13 ($n = 2$; data not shown) and 18 ($n = 4$; data not shown) confirmed that FGF-2 is not essential for cell proliferation during cerebral cortex development.

Possible defects in cortical layer morphogenesis were studied using an *in vivo* cell labeling system, which allows one to examine the migratory history of individual cells (reviewed by Bayer and Altman, 1991). This system takes advantage of the fact that the prospective target layer of a neuron normally is linked directly to its time of birth in the embryonic ventricular zone. Therefore, pregnant females were injected with BrdU at precise developmental time points to label pre-migratory neuronal cells. The fate of BrdU-positive neurons was analyzed ~1 month after birth on serial coronal sections of the rostral cerebral cortex (for details, see Material and methods). Pulse labeling at embryonic day 14.5–15 marks predominantly neuronal cells that colonize cortical layers III and II (Figure 4C), whereas cortical layers VI–IV are mostly

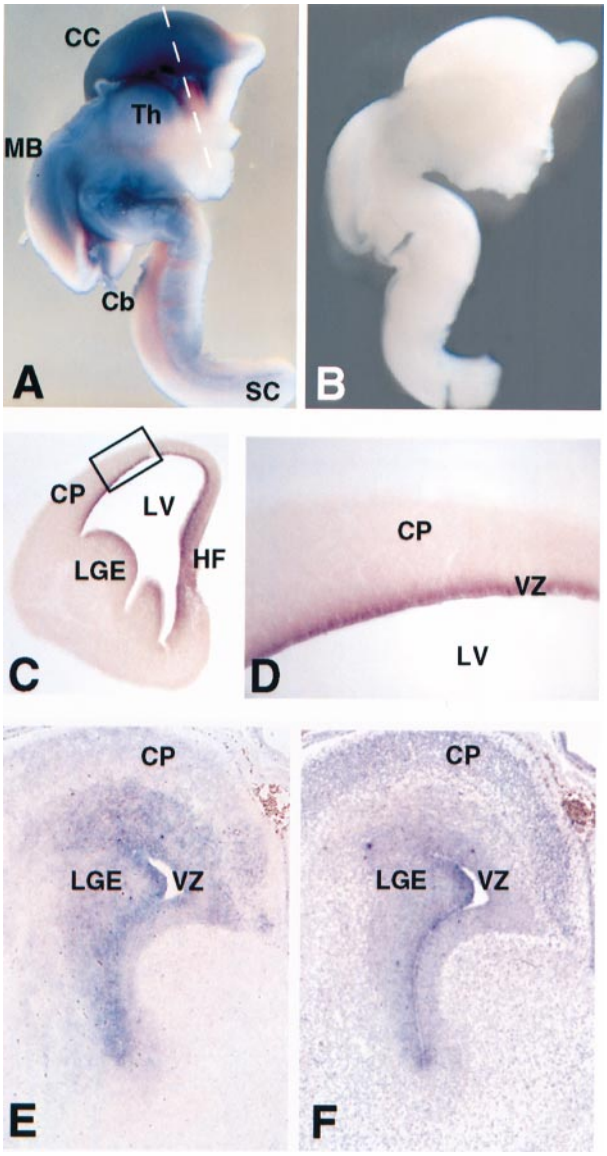

Fig. 2. Spatial distribution of FGF-2 and its cognate receptor isoforms during patterning of the cerebral cortex. (A–D) FGF-2 protein distribution in the CNS at embryonic day 14.5. (**A**) The isolated brain and attached spinal cord of a wild-type embryo were cut along the midline and FGF-2 proteins were detected by whole-mount antibody staining. The dashed white line indicates the approximate level of the coronal section shown in (C). (**B**) Whole-mount antibody staining of a CNS isolated from an age-matched FGF-2$^{-/-}$ litter mate. No staining is detected. (**C**) A rostral coronal cryosection (60 μm) of one cerebral hemisphere as indicated in (A). The rectangle indicates the approximate position of the enlargement shown in (D). (**D**) Magnification of the developing cortical plate and ventricular zone. FGF-2 levels are highest in the ventricular zone, where neuronal progenitors are born. (**E**) Distribution of transcripts encoding FGFR1 isoform IIIc in the ventricular zone and cortical plate of a wild-type embryo (embryonic day 16). (**F**) FGFR2 isoform IIIc transcripts in a section adjacent to the one shown in (E). The rostral positions of both sections (E and F) are similar to (C). Serial coronal sections (7 μm) were used to detect transcripts by non-radioactive RNA *in situ* hybridization (blue staining). Note that both FGF receptor isoforms are expressed at high levels in the ventricular and subventricular zones, whereas only FGFR2-IIIc expression persists in the cortical plate. Cb, cerebellum; CC, cerebral cortex; CP, cortical plate; HF, hippocampal formation; LGE, lateral ganglionic eminence; LV, lateral ventricle; MB, mid brain; SC, spinal cord; Th, thalamus; VZ, ventricular zone.

devoid of labeled cells in heterozygous adult mice (Figure 4C and D). In contrast, about twice as many labeled neuronal cells are located in the deeper cortical layers and corpus callosum of FGF-2-deficient mice (Table ID and E; $P < 0.05$; Figure 4E and F), indicative of their failure to reach target layers III and II. This defect is variable, as many more BrdU-positive cells (25–36%) are detected in corpus callosum and deep layers of the more severely affected FGF-2-deficient mice (*n*/total = 4/12; Figure 4E and F), whereas a few others are indistinguishable from controls (for details, see scatter plot, Table ID). This could be either a consequence of incomplete penetrance of the embryonic FGF-2 phenotype (see Discussion) or variable elimination of mislocalized cells by cellular apoptosis (see, for example, review by D'Mello, 1998). Concerning the latter, quantitative TUNEL analysis showed no significant differences in cell survival in either the embryonic (E16; $n = 5$), newborn ($n = 4$) or adult ($n = 4$) cerebral cortex (data not shown).

These defects should alter the distribution of specific neuronal populations. In particular, the distribution of the calcium-binding protein parvalbumin, which marks a significant number of neurons in several cortical layers (Celio, 1990), was analyzed in adult brains (Figure 4G–I). An average reduction of ~25% in parvalbumin-positive neurons is seen in FGF-2-deficient mice in comparison with controls (compare Figure 4H with I; see Table IF). This reduction affects all layers (Figure 4I and data not shown) and is comparable with the proportion of neuronal cells which fail to reach their target layers as estimated by BrdU pulse labeling (Table IE). In contrast, no differences in the distribution of glial fibrillary acidic protein (GFAP), which marks astroglial cells, were detected (data not shown). Furthermore, no striking behavioral abnormalities such as seizures (Chae *et al*., 1997) or *reeler*-like phenotypes (e.g. D'Arcangelo *et al*., 1995) were observed in FGF-2-deficient mice, although further tests are necessary to detect possible subtle defects.

Neuronal defects are not limited to the cerebral cortex

The hippocampal commissure, a brain region located beneath the cerebral cortex (Figure 5A and B), is devoid of parvalbumin-positive neurons in wild-type and heterozygous adult mice (Figure 5C; $n = 8$). However, FGF-2-deficient adult mice (*n*/total = 8/14) show varying degrees of ectopic parvalbumin-positive neurons in this region (Figure 5D). In contrast, the distributions of calbindin-positive neurons (Celio, 1990) and GFAP-positive glial cells were not altered (data not shown). Analysis of serial coronal sections of the adult spinal cord also revealed neuronal abnormalities throughout the mantle layer of the cervical region (Figure 5E–H; *n*/total = 5/12). Fewer differentiated large neurons (compare Figure 5H with G; arrowheads in Figure 5H) were observed, whereas all other neural cell types appear normal (arrows in Figure 5H). These studies indicate that FGF-2 also functions in subcortical and spinal cord neurons in agreement with its expression by the hippocampal formation (Figure 2C) and embryonic spinal cord (Figure 2A, see also Dono and Zeller, 1994).

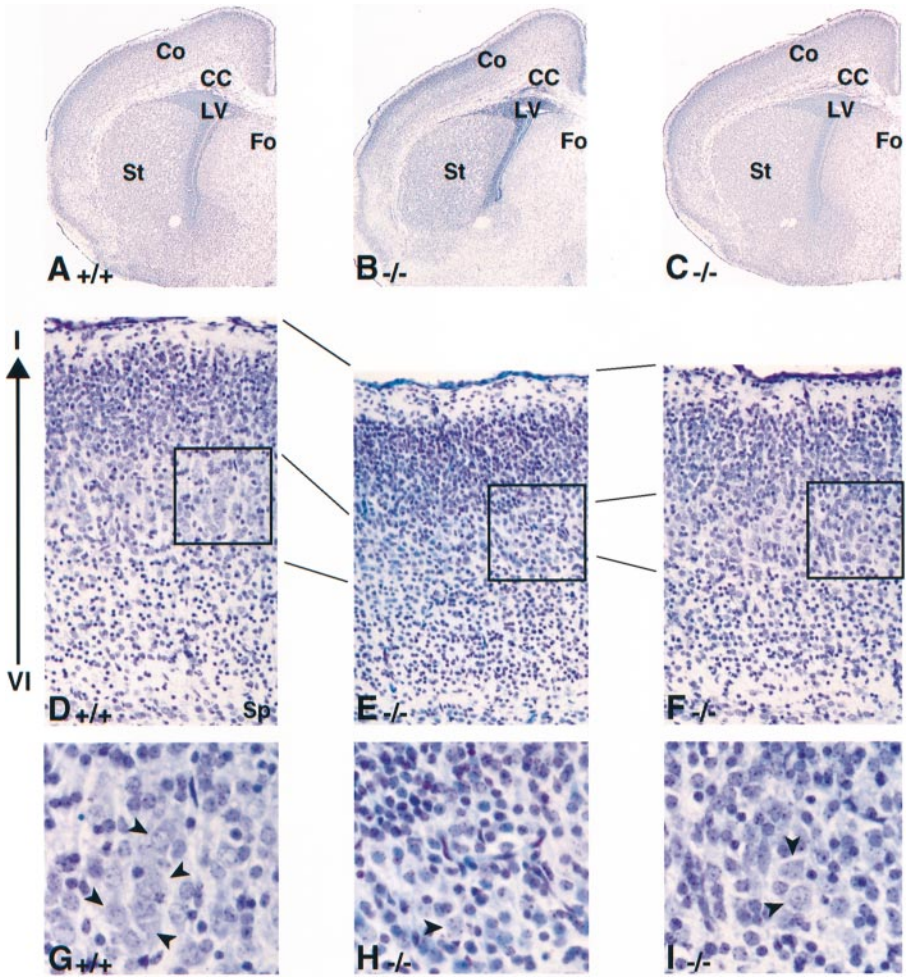

Fig. 3. Compression of cortical layers and pyramidal neuron deficiencies in FGF-2-deficient mice at birth. (**A**–**C**) Serial coronal sections (7 μm paraffin) of the rostral brain (somato-sensory cerebral cortex, only one hemisphere shown) were analyzed by Nissl staining. (A), (D) and (G) Brain of a wild-type newborn mouse. (B), (E) and (H) Brain of an FGF-2-deficient mouse with only few differentiated pyramidal neurons (see H). (C), (F) and (I) Brain of another FGF-2-deficient mouse. (**D**–**F**) Enlargement of the parietal region of the cerebral cortex. The arrow indicates the polarity of the cerebral cortex layers (VI, deepest layer; I, most superficial layer). (**G**) Enlargement of the pyramidal neuron layer (arrowheads) in the wild-type. (**H**) Enlargement of the corresponding region in an FGF-2-deficient cerebral cortex. The arrowhead indicates the only cell within the field reminiscent of a pyramidal neuron. The small nuclei most likely correspond to cells located normally more superficially (compare D with E), which reflects the compression and mixing of the cortical layers. (**I**) Enlargement of the homozygous cerebral cortex shown in (F). (H) and (I) are representative of the range of pyramidal neuron deficiencies detected at birth. CC, corpus callosum; Co, differentiating cortex; Fo, fornix; LV, lateral ventricle; Sp, subplate; St, striatum.

Reduced blood pressure and impaired baroreflex function in FGF-2-deficient mice

Exogenous administration of FGF-2 induces hypotensive effects in rats, rabbits and dogs (Cuevas *et al*., 1991; Lazarous *et al*., 1995), suggesting possible antihypertensive actions of endogenous FGF-2 proteins (Cuevas *et al*., 1996). Therefore, the resting blood pressure of adult FGF-2-deficient mice was determined and compared with that of wild-type (+/+) and heterozygous (+/–) litter mates to uncover possible FGF-2 functions in blood pressure control. Initial statistical evaluation of resting blood pressure recordings showed that no differences are observed between wild-type and heterozygous mice (data not shown). Therefore, these two genotypes (+/+; +/–) served as phenotypic controls. However, studies by Krege *et al*. (1995) revealed a gender difference in blood pressure levels using wild-type mice of a similar genetic background to the present studies (mixed C57BL/6J×129/Sv). In agreement with these studies, male control mice display on average an ~14 mmHg higher blood pressure than females (compare Figure 6B with A).

Analysis of the primary recordings of female FGF-2-deficient mice (Figure 6A) reveals a significant decrease in resting blood pressure in comparison with wild-type and heterozygous female litter mates (Figure 6B). Similarly, many FGF-2-deficient males (Figure 6B) also display lower resting blood pressures than their wild-type litter mates, but a substantial fraction (*n*/total = 4/12) have elevated blood pressures (see scatter plot, Figure 6B). This variation could be caused by incomplete penetrance of the phenotype or unknown modifiers of blood pressure in males. To assess the effects of the FGF-2 deficiency on blood pressure independent of gender, the blood pressure differences (Δ blood pressure, Figure 6C and D) were calculated by subtracting the mean value of the respective control group (+/+; +/–) from the individual recordings.

Table I.

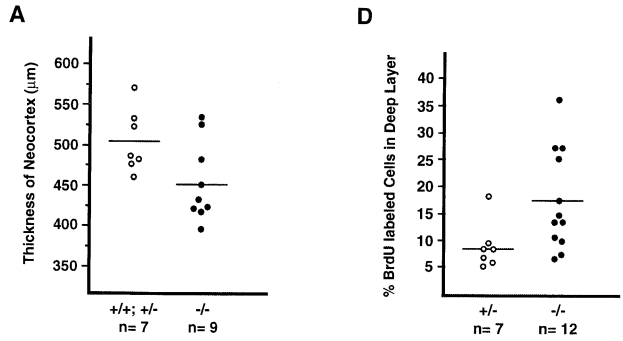

B

Thickness of Neocortex

Genotype	N	Thickness (μm)
+/+; +/-	7	504 ± 40
-/-	9	455 ± 48*

E

% BrdU labeled Cells in Deep Layers

Genotype	N	Percentage
+/-	7	8.8 ± 4.4
-/-	12	17.3 ± 9.3*

C

BrdU labeled Cells in the Dorsal Ventricular Zone (E 14.5 - 15)

Genotype	N	Average No.
+/+	4	306 ± 22
-/-	4	312 ± 21

F

Numbers of Parvalbumin positive Neurons per Hemisphere

Genotype	N	Average No.
+/+; +/-	6	851 ± 69
-/-	5	657 ± 82*

(**A**) Scatter plot showing the thickness (μm) of the neocortex in wild-type, heterozygous and FGF-2-deficient newborn litter mates. Lines in the scatter plots indicate the average measurements given in (B). (**B**) Average thickness of the neocortex (± SD). *P <0.05. (**C**) The average numbers of proliferating neuronal progenitors in the dorsal part of the ventricular zone were determined for wild-type and FGF-2-deficient embryos (E14.5–15). No significant differences in proliferation of neuronal progenitors are observed. Calculation of the 90% confidence interval (280–332) showed that proliferation differences >8% would have been reliably detected. (**D**) Scatter plot showing the percentage of BrdU-positive cells remaining in the deeper cortical layers (VI–IV) and the corpus callosum of adult heterozygous and FGF-2-deficient litter mates. Lines in the scatter plots indicate the average percentage given in (E). (**E**) Average numbers of BrdU-positive cells (± SD) remaining in the deeper cortical layers (VI–IV) and the corpus callosum. *P <0.05. (**F**) Parvalbumin-positive neurons are indicated as mean numbers (± SD) per cerebral cortex hemisphere. *P <0.002.

Analysis of the resulting histograms (including all mice from both sexes, Figure 6C and D) shows that the blood pressure differences of control mice are distributed normally around zero (Figure 6C). In contrast, the distribution is shifted by about –10 mmHg in FGF-2-deficient mice (Figure 6D). On average, the blood pressure of FGF-2-deficient adult mice is reduced by ~10 mmHg in comparison with control litter mates (P <0.02).

This hypotensive phenotype might be the result of an insufficiency affecting smooth muscle and/or myocardial function (see Introduction). If this were the case, then the hypotensive phenotype should be aggravated further by chronic elevation of blood pressure. Therefore, hypertension was induced in FGF-2-deficient and control mice by continued infusion (6 days) of angiotensin II, which causes vasoconstriction and induces myocardial growth (Kim *et al.*, 1995). As shown in Figure 7A, FGF-2-deficient mice respond to chronic angiotensin II infusion with an even more pronounced increase in blood pressure than controls (control, 19 ± 14 mmHg; –/–, 30 ± 13 mmHg; P = 0.05) to reach identical hypertensive levels. No differences in baseline plasma renin values, heart rates and body weights were observed between control and FGF-2-deficient mice (data not shown). These results demonstrate that FGF-2-deficient mice retain the ability to induce and maintain elevations of blood pressure in response to an exogenous vasoconstrictor such as angiotensin II.

Reduced blood pressure in combination with intact responsiveness to exogenously induced vasoconstriction is a common manifestation in autonomic dysfunction, which is characterized by an impaired baroreceptor reflex response to hypotensive stimuli (Bannister, 1988). To assess neuronal control of blood pressure in FGF-2-deficient mice, acute peripheral vasodilatation was induced by intravenous infusion of isoproterenol, a β1/β2-adrenoreceptor agonist. The response to different doses of isoproterenol was determined in a pilot experiment using six male control mice (see Materials and methods). As expected, heart rates increased in a dose-dependent fashion (data not shown), whereas blood pressure remained at its baseline value (Figure 7B) during administration of isoproterenol up to 0.05 ng/g body weight/min, indicating intact baroreceptor reflex regulation. Subsequently, the effects of this dose were studied in FGF-2-deficient male mice with a resting blood pressure <135 mmHg (Figure 7C and D). In contrast to the controls (Figure 7B), the blood pressure declined with a characteristic time course in FGF-2-deficient litter mates (Figure 7C). A significant drop in blood pressure was observed in all homozygous mutants but not in control mice (Figure 7D). Furthermore, while heart rates increased as expected in control male mice (Δ: +42 ± 35 beats/min), they failed to increase in FGF-2-deficient litter mates (Δ: –13 ± 34 beats/min; P <0.02). Taken together, these studies indicate that neural reflex control of blood pressure is impaired in FGF-2-deficient mice.

Discussion

FGF-2 is required for normal CNS development

FGF-2-deficient mice display neurological defects consistent with essential functions during development of the CNS. In particular, lack of FGF-2 signaling affects migration of a fraction of neuronal precursors during cerebral cortex development (see below). Lack of FGF-2 also induces ectopic parvalbumin-positive neurons in the hippocampal commissure and results in neuronal deficiencies affecting the cervical spinal cord. Previous studies suggested major roles for FGF-2 in glial cell proliferation and survival (see, for example, Petroski *et al*., 1991; Qian *et al*., 1997). The present genetic analysis failed to reveal defects in astroglial cells, suggesting that the cellular defects primarily affect neuronal cell types. Furthermore, an autonomic dysfunction impairing blood pressure regulation points to general roles in neural development and function. Previous studies using cultured CNS progenitors have suggested a major role for FGF-2 signaling in cell proliferation (Temple and Qian, 1995). However, the present study establishes that neuronal proliferation is normal during cerebral cortex morphogenesis in FGF-2-deficient embryos. Therefore, FGF-2 either does not function as a mitogenic signal for neural progenitors or its deficiency is functionally compensated by other FGFs *in vivo*. Indeed, several other FGFs are expressed by

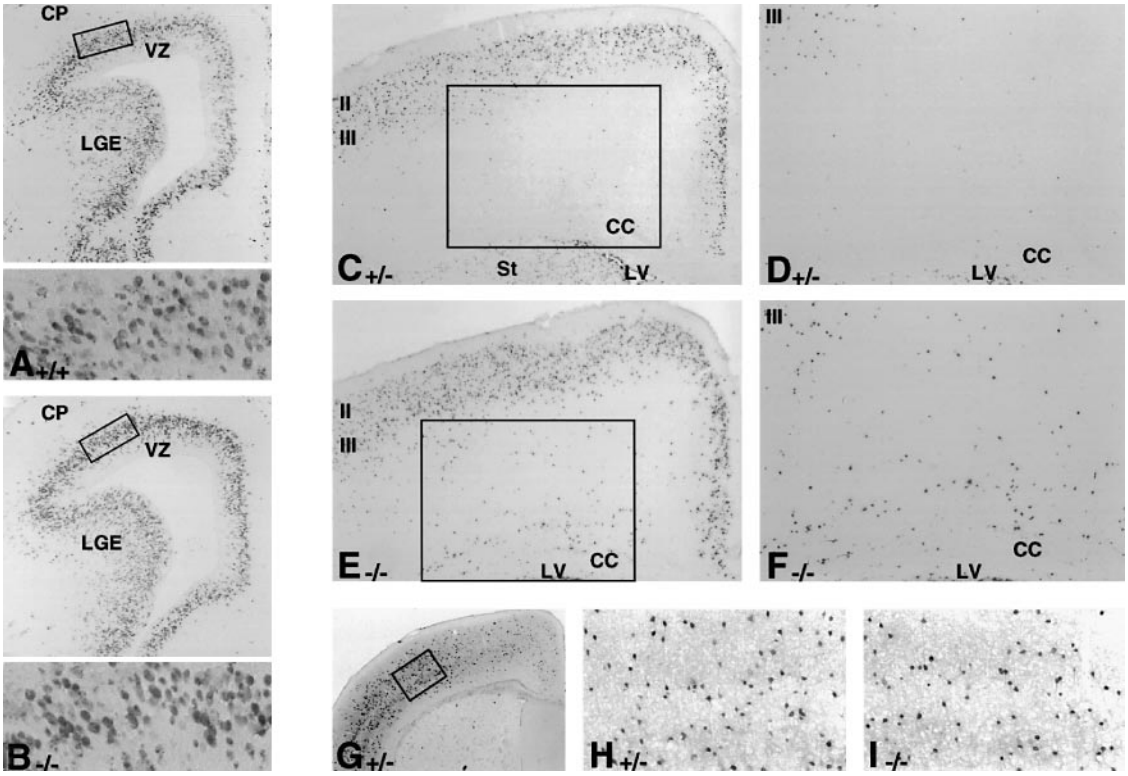

Fig. 4. A fraction of neuronal progenitors fail to colonize their target layers during cerebral cortex morphogenesis. (**A**) and (**B**) Proliferation of neuronal progenitors during embryonic day 14.5–15 as visualized by BrdU incorporation. Coronal sections show proliferating cells in the ventricular zone of the lateral ventricle (positions are similar to those shown in Figures 2C–F). (A) Wild-type embryo, (B) homozygous litter mate. Insets in (A) and (B) show an enlargement of the lateral aspects of the dorsal ventricular zone as indicated by rectangles. (C–F) Migration of neuronal precursors to cortical layers III and II was studied by injecting pregnant females with BrdU between embryonic days 14.5 and 15. The distribution of BrdU-labeled neuronal cells was analyzed 4–5 weeks after birth on serial coronal cryosections using specific antibodies. Sections from the somatosensory part of the rostral cerebral cortex are shown. (**C**) Rostral cortex section of a heterozygous brain. (**D**) Enlargement to show the deeper cortical layers and corpus callosum. Note that very few labeled cells are present in this region of the control cortex. (**E**) Rostral cortex section of an FGF-2-deficient brain with ~27% of all BrdU-positive cells remaining in layers IV–VI and the corpus callosum. (**F**) Enlargement to show BrdU-labeled cells remaining in the deeper cortical layers and corpus callosum of the FGF-2-deficient brain. The rectangles in (C) and (E) indicate the approximate position of (D) and (F). (G–I) Distribution of parvalbumin-positive neurons in a control (**G** and **H**) and FGF-2-deficient cerebral cortex (**I**). The rectangle in (G) indicates the approximate position of the enlargements shown in (H) and (I). II, cortex layer II; III, cortex layer III; CC, corpus callosum; CP, cortical plate; LGE, lateral ganglionic eminence; LV, lateral ventricle; St, striatum; VZ, ventricular zone.

the ventricular zone of the developing cerebral cortex, including FGF-1, the closest relative of FGF-2 (Wilcox and Unnerstall, 1991). It is possible that FGF-1 compensates and/or acts as a mitogenic signal for neural progenitors. Functional compensation may also account for the variable and/or rather restricted phenotypes observed in FGF-2-deficient mice. Indeed, it has been proposed that such compensation could account for both incomplete penetrance and restricted phenotypes observed in mouse embryos deficient for either FGF receptors (see, for example, FGFR1: Yamaguchi *et al*., 1994) or specific ligands (see, for example, FGF-3: Mansour *et al*., 1993; FGF-5: Hebert *et al*., 1994). However, the identification of shared functions has to await further genetic study and analysis of compound mutant embryos. Alternatively, phenotypic variation could be caused by non-uniform segregation of unknown modifiers in a mixed genetic background.

Genetic evidence that FGF-2 participates in regulating fate, migration and differentiation of neuronal progenitors

The neuronal precursors of the cerebral cortex are generated in the ventricular zone, and glial fibers provide a generic guide for radial migration to their target layers (reviewed by Hatten, 1993). One of the earliest determinative events of cortical layer formation is the colonization of layer I by Cajal–Retzius (CR) neurons, which promote differentiation of radial glial cells prior to the onset of neuronal migration (Soriano *et al*., 1997). CR neurons produce reelin, an extracellular matrix protein, whose disruption by the murine *reeler* mutation causes inversion of all cortical layers (D'Arcangelo *et al*., 1995). Several additional components of a genetic cascade controlling establishment of the cortical plate and migration of neuronal precursors have been identified. Inactivation of mouse *disabled-1*, a component of the Src signal transduction cascade, Cdk5 and p35, which are all expressed by neuronal cells, also resulted in *reeler*-like phenotypes (Ohshima *et al*., 1996; Chae *et al*., 1997; Howell *et al*., 1997). Therefore, these genes could be part of the same or parallel signaling pathways, which regulate cell migration and organization of the cerebral cortex.

These mutations, however, do not seem to alter neuronal cell fates, which are specified during the final cell divisions in the ventricular zone (reviewed by Bayer and Altman, 1991; see also Howell *et al*., 1997). The migratory path of a neuronal progenitor is defined by cell–cell interactions

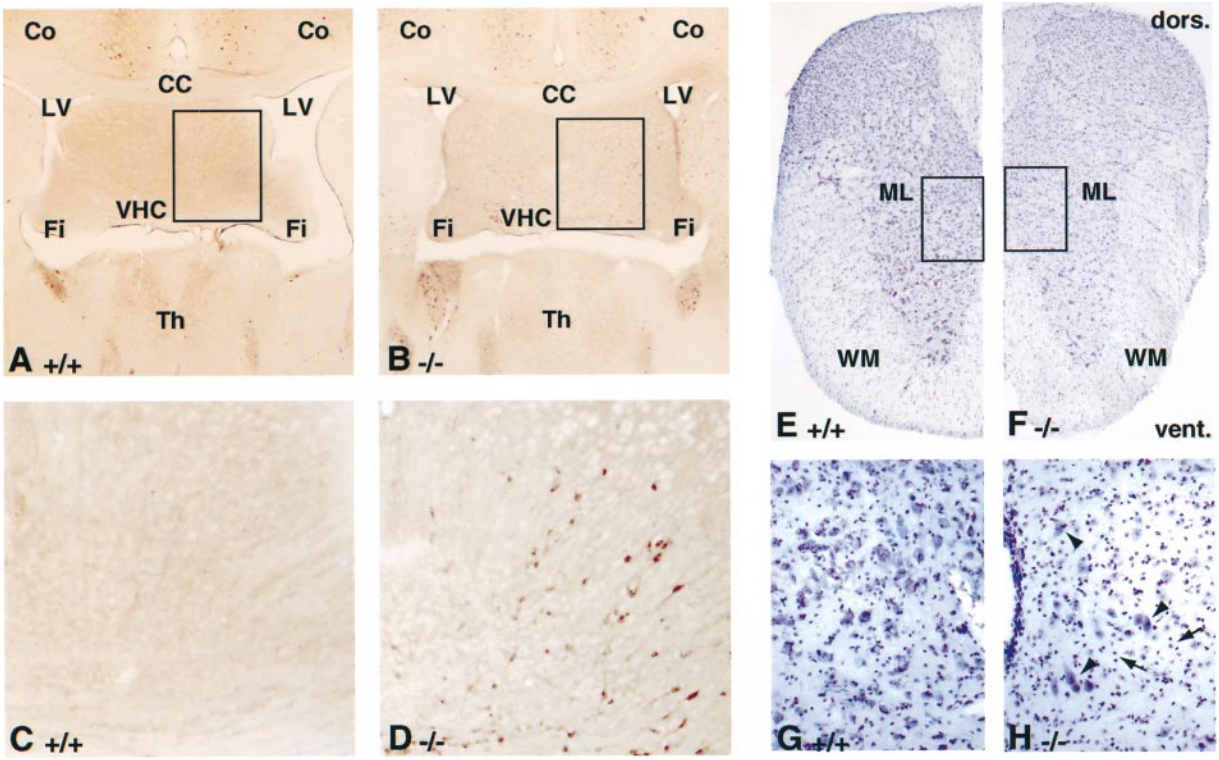

Fig. 5. Neuronal defects in other CNS areas of FGF-2-deficient mice. (A–D) Ectopic parvalbumin-positive neurons are present in the region of the hippocampal commissure in FGF-2-deficient adult brains. Parvalbumin-positive neurons were detected on serial coronal cryosections using specific antibodies. (**A**) Low magnification to show the area of the hippocampal commissure in a wild-type brain. This section is located rostral to the hippocampus. (**B**) A comparable area of an FGF-2-deficient brain. The rectangles in (A) and (B) indicate the approximate positions of (C) and (D). (**C**) The wild-type hippocampal commissure does not contain parvalbumin-positive neurons. (**D**) In contrast, many parvalbumin-positive neurons are present in the corresponding region of the FGF-2-deficient brain. (E–H) Neuronal deficiencies in the spinal cord of adult FGF-2-deficient mice. Serial transversal sections of the cervical spinal cord (C2) were analyzed following Nissl staining. (**E**) Wild-type spinal cord with well differentiated neurons in its mantle layer. (**F**) A comparable section of a homozygous mutant spinal cord with a less distinct mantle layer containing fewer neurons. The rectangles indicate the approximate positions of (G) and (H). (**G**) Enlargement showing many large and well differentiated neurons in the wild-type spinal cord. (**H**) Only small clusters of differentiated large neurons (arrowheads) are present in the mutant spinal cord. Other neural cell types appear normal (arrows). CC, corpus callosum; Co, cortex; dors., dorsal; Fi, fimbria; LV, lateral ventricle; ML, mantle layer; Th, thalamus; vent., ventral; VHC, ventral hippocampal commissure; WM, white matter.

and exposure to unknown signals during its cell fate determination within the ventricular zone (reviewed by Hatten, 1993). The present genetic study indicates that FGF-2 is one of these signals as its expression is highest in the ventricular zone and a fraction of neuronal progenitors fail to reach their target layers in FGF-2-deficient mice. Therefore, FGF-2 most likely participates in defining both the cell fate (see also Ghosh and Greenberg, 1995; Vicario-Abejon *et al*., 1995) and migratory path of neuronal progenitors. As Src family kinases can transduce FGF-2 signals (Zhan *et al*., 1994; Yayon *et al*., 1997), it is possible that FGF-2 is part of a common signaling cascade involving both rather general (*reeler*-like, see above) and specific cues (such as FGF-2) to regulate neuronal cell migration directly during cortical layer formation.

Our genetic study also reveals that ectopic parvalbumin-positive neurons are present in hippocampal commissure of FGF-2-deficient mice. Therefore, FGF-2 normally should function to suppress differentiation of parvalbumin-positive neurons in the hippocampal commissure. Indeed, previous studies indicated that FGF-2 levels might control the fate and differentiation of cultured cortical stem cells (Ghosh and Greenberg, 1995; Qian *et al*., 1997). Low levels of FGF-2 promote neuronal differentiation, possibly in combination with other factors such as neurotrophins (Temple and Qian, 1995), while high levels induce glial cell types (Qian *et al*., 1997). Therefore, our genetic analysis shows that FGF-2 functions in the control of neuronal cell fates and/or differentiation, whereas it is not essential for proliferation.

An evolutionarily conserved function of FGF signaling in regulating embryonic cell migration

Genetic analysis in the mouse demonstrated a role for FGFR1 signaling in the morphogenetic movements of mesodermal cells through the primitive streak (Yamaguchi *et al*., 1994). Furthermore, expression of a dominant-negative FGFR1 transgene in oligodendrocyte precursors disrupted their migration in newborn brains (Osterhout *et al*., 1997). Our analysis of FGF-2-deficient embryos demonstrates that FGF signaling controls aspects of cell migration during patterning of the vertebrate neocortex. In *Drosophila*, FGF signaling also controls morphogenetic movements such as those occurring during gastrulation, neurogenesis and tracheal development (Klämbt *et al*., 1992; Gisselbrecht *et al*., 1996). Interestingly, the FGF ligand *branchless* (Sutherland *et al*., 1996) seems to act

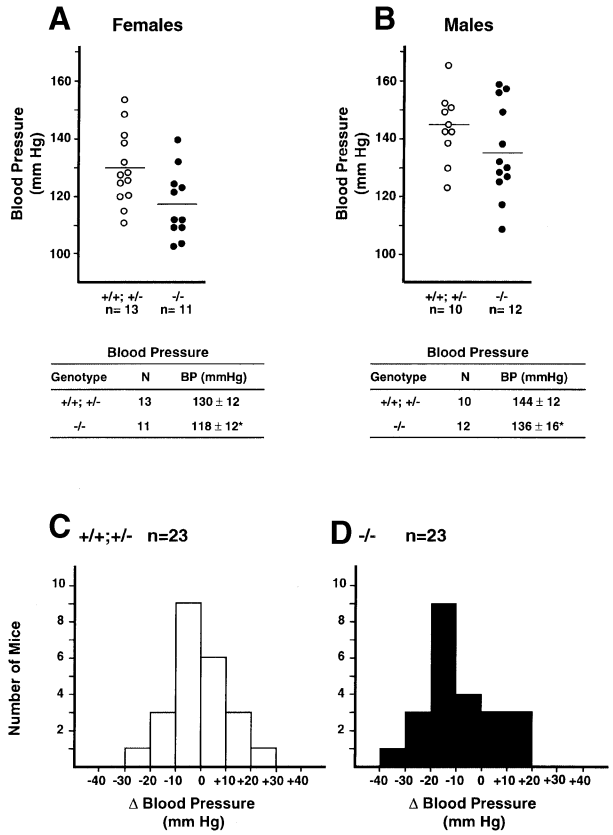

Fig. 6. Analysis of resting blood pressure levels. (**A**) Scatter plots showing the resting blood pressures in awake female control (+/+ and +/–; ○) and FGF-2-deficient (–/–; ●) mice. Group mean values are indicated by lines. Table: group mean values (± SD) of control and FGF-2-deficient females. **P* <0.05. (**B**) Scatter plots showing resting blood pressures in awake male control (+/+ and +/–; ○) and FGF-2-deficient (–/–; ●) mice. Group mean values are indicated by lines. Table: group mean values (± SD) in control and FGF-2-deficient males. **P* <0.2. BP, mean arterial blood pressure. (**C**) Histogram showing the distribution of individual blood pressure differences (Δ blood pressure) in control mice of both sexes (+/+ and +/–; open bars). (**D**) Histogram showing the distribution of individual blood pressure differences in FGF-2-deficient mice of both sexes (–/–; filled bars). For details of statistical evaluation, see Results.

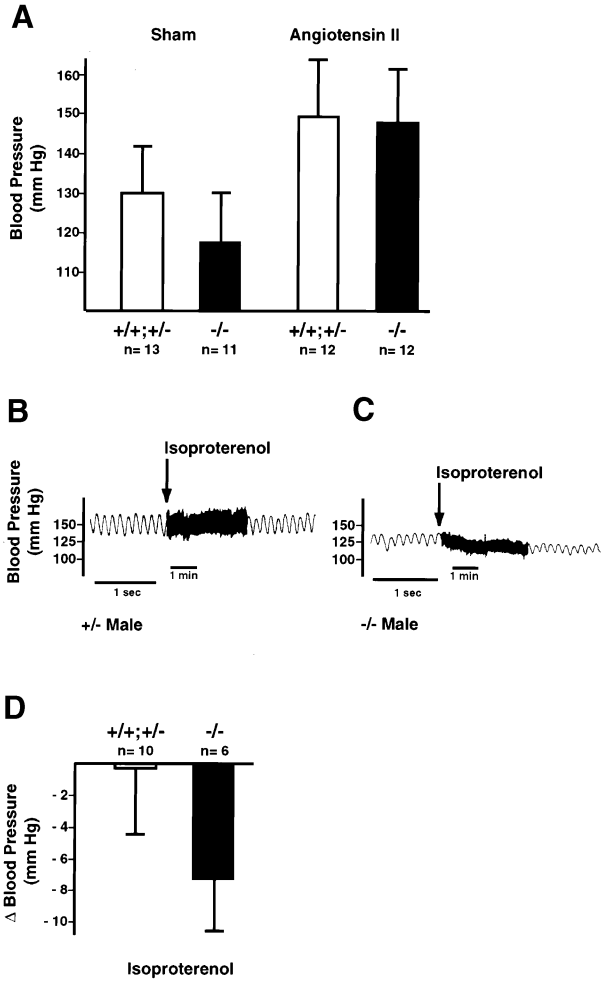

Fig. 7. Adult FGF-2-deficient mice respond normally to chronic angiotensin II infusion but show an impaired baroreceptor reflex. (**A**) Effects of continuous angiotensin II infusion over 6 days on resting blood pressure in awake control (+/+ and +/–; open bars) and FGF-2-deficient (–/–; filled bars) female mice. Sham-treated mice did not receive angiotensin II. In both groups of angiotensin II-infused mice, blood pressure was significantly increased to about the same absolute level ($P < 0.01$). All values are means ± SD. (B–D) Effects of isoproterenol infusions on resting blood pressure in awake control and FGF-2-deficient male mice. (**B**) Typical recording in a heterozygous mouse. (**C**) Typical recording in an FGF-2-deficient mouse. The arrows in (B) and (C) indicate the time when the isoproterenol infusion was started. (**D**) Average responses to isoproterenol in control (+/+ and +/–; open bar) and FGF-2-deficient (–/–; filled bar) mice. The resting blood pressure (measured as mean arterial blood pressure) was significantly reduced ($P < 0.02$) by isoproterenol in FGF-2-deficient but not in control mice. All values are means ± SD.

as a chemoattractant to guide migration of tracheal cells expressing the cognate FGF receptor *breathless* (Klämbt *et al*., 1992). In contrast, during vertebrate neocortex layer formation, neurons are exposed to FGF-2 signals prior to or during onset of migration to their target layers as no protein is detected in the cortical plate. Therefore, it is unlikely that FGF-2 functions as a chemoattractant (see also Armstrong *et al*., 1990). These distinct modes of action probably reflect mechanistic differences in the underlying morphogenetic movements. Indeed, neurons moving along radial glial fibers use different cell adhesion and cytoplasmic streaming mechanisms than, for example, migrating neural crest cells (discussed by Fishell and Hatten, 1991). Therefore, FGF-2 most likely regulates migration indirectly by modulating the adhesive properties of neuronal cells as evidenced by previous studies of neuroepithelial cells in culture (Kinoshita *et al*., 1993). In summary, genetic analysis of FGF ligands and receptors in different species points to general roles for FGF signaling in cell migration during embryogenesis.

An autonomic dysfunction affects blood pressure regulation in FGF-2-deficient mice

FGF-2-deficient adult mice display a lower blood pressure than their wild-type or heterozygous litter mates. Recently, Zhou *et al*. (1998) also reported a similar hypotensive phenotype independently derived in FGF-2-deficient mice. These genetic observations are rather surprising as previous studies demonstrated that exogenous FGF-2 induces hypotension in normotensive and hypertensive animals (Cuevas *et al*., 1991; Lazarous *et al*., 1995). Furthermore, reduction of endogenous FGF-2 levels in endothelial cells was correlated to elevated blood pressure in spontaneously

hypertensive rats, a genetic model for studying hypertension (Cuevas *et al*., 1996). Accordingly, one might expect increased blood pressure levels rather than a hypotensive phenotype in FGF-2-deficient mice. A possible explanation for this apparent discrepancy may be that signaling by endogenous FGF-2 does not affect blood pressure directly under normal physiological conditions. In the cardiovascular system, the major stimulus for FGF-2 release appears to be transiently increased cell membrane permeability (Clarke *et al*., 1995; Kaye *et al*., 1996). Indeed, recent observations indicate that FGF-2 release from vascular smooth muscle cells requires mechanical strains well above the physiological range of normal arteries (Cheng *et al*., 1997). Thus, only under pathophysiological conditions associated with elevated mechanical strain, such as hypertension, may the endogenous release of FGF-2 be sufficiently high to lower blood pressure. Such an interpretation would also explain the exaggerated increase in blood pressure in FGF-2-deficient mice during chronic angiotensin II infusion.

In fact, several of our observations indicate that the reduced blood pressure in FGF-2-deficient mice is a consequence of an autonomic dysfunction, which characteristically is associated with hypotension (Bannister, 1988). First, FGF-2-deficient mice show an exaggerated increase in blood pressure in response to an exogenous vasoconstrictor (see above). This observation argues strongly against a chronic smooth muscle and/or myocardial insufficiency being the primary cause of the reduced blood pressure. Second, an acute vasodilatory stimulus (isoproterenol), which does not trigger a hypotensive response in control mice, induces a drop in blood pressure in FGF-2-deficient mice. This response, together with an impaired increase in heart rates, indicates that vasodilatation is not compensated by increased sympathetic nerve activity, a phenomenon observed in most human patients with autonomic failure (Mathias, 1988). Finally, FGF-2 is expressed by the intermediolateral autonomic nuclei (Stapf *et al*., 1997) in the spinal cord. Even though preliminary analysis failed to reveal striking reductions in the numbers of pre-ganglionic sympathetic neurons, neuronal lesions were observed in various other CNS regions in FGF-2-deficient mice. Such neuronal deficiencies have been reported in human patients with autonomic failure and are clinically defined as 'multiple system atrophy' (Bannister, 1988).

Further studies will be necessary to define at which cellular and/or molecular level the neural control of blood pressure is impaired in FGF-2-deficient mice. Despite the fact that most clinical cases of autonomic failure in humans are secondary forms with a different pathogenesis (Bannister, 1988), FGF-2-deficient mice appear to be the first defined genetic model of autonomic dysfunction. These mice will enable embryological, cellular and physiological analyses of normal and pathological development of the autonomic innervation and neural regulation of blood pressure.

Materials and methods

Targeting vector and generation of FGF-2-deficient mice

Genomic clones were isolated by screening a 129/Sv λ phage library (provided by R.Klein) with a cDNA probe encoding the ATG-initiated FGF-2 isoform (Hebert *et al*., 1990). A 15 kb genomic clone spanning the first FGF-2 coding exon was used to generate the targeting construct in a pPNT-based vector (Figure 1A, Tybulewicz *et al*., 1991; provided by R.Klein). An 8 kb fragment of intronic sequences upstream of the first coding exon (long arm) was inserted into the *Sal*I restriction site located between the PGK-neo and PGK-tk marker genes. Subsequently, a 1.5 kb fragment of intronic sequences located downstream of the exon (short arm) was inserted into an *Xho*I–*Not*I restriction site vector. Therefore, the resulting targeting construct induces replacement of a 2.3 kb fragment containing the first FGF-2 coding exon by the PGK-neo gene in the opposite transcriptional orientation (Figure 1A). Transfection and selection of correctly targeted R1-ES cells (Nagy *et al*., 1993) were performed as previously described (Wurst and Joyner, 1993). PCR-positive ES cell clones were obtained and accurate targeting was confirmed by Southern blotting. Five to 10 μg of genomic DNA was digested with *Pst*I and probed with a genomic fragment located immediately downstream of the 3′ end of the short arm (Figure 1C), a neo probe and a 5′ probe. Three correctly targeted clones were injected into C57BL/6J blastocysts as previously described (Wurst and Joyner, 1993) and chimeras from one clone resulted in germline transmission. Mice were genotyped either by PCR using specific oligos or by Southern blotting. Mice of mixed C57BL/6J×129/Sv backgrounds were generated as follows: chimeras (composed of ES cells of 129/Sv background) were crossed to C57BL/6J females and their heterozygous (+/–) F_1 progeny crossed to generate all three genotypes. These mice and subsequent offspring were used for all studies. Litter mates of the same genotype always contributed randomly to the data points obtained by analyzing several litters. The statistical significance of all phenotypic differences between control and FGF-2-deficient mice was validated using the unpaired Student's *t*-test.

Immunoblot analysis of FGF-2 proteins

Immunoblot analysis was performed as previously described (Dono and Zeller, 1994) with the exception that ECL detection was used (Amersham). FGF-2 proteins were detected using affinity-purified polyclonal FGF-2 antibodies (Dono and Zeller, 1994).

Whole mount antibody and section RNA in situ analysis

Embryos were collected and genotyped using DNA prepared from extra-embryonic membranes. Brains were dissected in ice-cold phosphate-buffered saline (PBS), cut along the medial plane into left and right hemispheres and processed for whole-mount antibody staining as previously described (Riese *et al*., 1995). Alternatively, heads were isolated and paraffin embedded for subsequent RNA *in situ* hybridization analysis on sections. Coronal sections (6 μm) were processed and hybridized using digoxigenin-labeled riboprobes as described (Neubuser *et al*., 1997). Riboprobes for FGFR1 (450 bp PCR fragment) and FGFR2 (360 bp) are complementary to the isoform-specific sequences encoding the immunoglobulin domain IIIc (plasmids provided by G.Holländer; unpublished).

Histological analysis

Newborn mice were decapitated and their heads fixed for ~12 h in 4% phosphate-buffered paraformaldehyde (4% PFA) at 4°C. Adult mice were perfused with 4% PFA, and dissected heads and spinal cords were fixed overnight at 4°C. Subsequently, brains and spinal cords were dissected from skulls and bones, fixed for an additional 12–24 h and then either embedded in paraffin wax (newborns) or processed for cryo-sectioning (adults). For cryo-sectioning, the fixative was replaced with 30% sucrose in PBS and tissues were cryo-protected in tissue freezing medium (Tissue-Tek) prior to sectioning. Serial (7 μm, paraffin wax) or coronal (25 μm, frozen) sections were mounted on gelatin-coated slides and dried at 42°C or at room temperature. Sections were stained subsequently with 0.1% cresyl violet (Nissl-stain).

Measurement of cerebral cortex thickness at birth

The thickness of the cerebral cortex was determined using Nissl-stained coronal brain sections (7 μm, paraffin). Measurements of the frontal cortex were done using sections at identical antero-posterior positions. Duplicate measurements of both hemispheres were made ~80 μm apart. Variations among the measurements from one brain were $<5\%$ in all cases.

BrdU labeling of embryos for cell proliferation studies

At defined developmental time points, pregnant females were injected intraperitoneally with BrdU solution (7.5 μg/g body weight, Sigma) and sacrificed 1 h later. BrdU-labeled nuclei were detected as described

below. Proliferating cells were quantitated using age-matched wild-type and homozygous litter mate embryos. Four equally spaced coronal sections were analyzed per brain. BrdU-positive cells in the dorso-lateral aspect of the ventricular zone in both brain hemispheres were counted using an ocular micrometer to permit quantitation of equal squares.

Cell migration studies

In a series of pilot experiments, embryos were BrdU pulse-labeled between embryonic days 12 and 16 to study cell migration during cortical layer formation. These initial studies established that progenitors labeled between embryonic days 14.5 and 15 colonize predominantly layers III and II, while deeper cortical layers VI–IV are mostly devoid of labeled cells. Accordingly, cells which fail to migrate to their target layers and remain in deeper layers can be identified readily. In contrast, during earlier developmental stages (embryonic days 14 and earlier), cells colonize predominantly cortical layers VI–IV, which renders detection of only a fraction of mis-localized neuronal cells impossible (data not shown). Therefore, pregnant females between embryonic days 14.5 and 15 were injected with BrdU. Offspring were analyzed 4–5 weeks postnatally to ensure that cell migration and cortical layer formation were completed (Bayer and Altman, 1991). Heterozygous females were crossed with homozygous males to enable comparison of a large number of heterozygous offspring with homozygous litter mates. Only litters in which all brains of both genotypes showed predominant labeling of cortical layers II and III (assessed by comparison with Nissl-stained parallel sections) were included in the analysis shown in Table ID and E. Anesthetized mice were perfused and processed for cryo-sectioning as described before. Serial coronal sections (25 μm) were collected individually in PBS. Sections were incubated free-floating in solution and endogenous peroxidases were blocked by treatment with 2% H_2O_2 in H_2O for 15 min. Subsequently, sections were pre-treated in 2 M HCl solution (1 h at 37°C), trypsin digested (5 mg/ml for 6 min at room temperature) and permeabilized with Tween-20 (0.5% in PBS for 20 min at room temperature). Following washing in PBS and post-fixation in 4% PFA, sections were blocked in 5% goat serum, 3% bovine serum albumin (BSA) and 0.3% Tween-20 in PBS (BS) for 1 h at room temperature. Incubation with antibodies was done overnight at 4°C (1 U/ml in BS). Immune complexes were visualized using 1 mg/ml diaminobenzidine tetrahydrochloride (Sigma) and 0.03% H_2O_2 (Aldrich) in 0.1 M Tris pH 7.2. Afterwards, sections were mounted on gelatin-coated glass slides, dried overnight at room temperature and mounted in Eukitt medium (Riedel-de-Haën).

Quantitation of cell migration experiments and parvalbumin-positive neurons

In 4- to 5-week-old mice, large round nuclei (indicative of neurons) were counted in the target layers III and II and the area between lateral ventricle and cortex layer III using an ocular micrometer to enable quantitation of equal squares. Both left and right cortical hemispheres were analyzed using four sections spaced at roughly equal intervals in the anterior part of either heterozygous or FGF-2-deficient mice. For each cerebral cortex, the cells which fail to colonize their target layers (i.e. positive cells remaining in the corpus callosum and layers VI–IV) were determined as a percentage of the positive cells in target layers III and II (Table IE). Weakly labeled small or irregular nuclei were not counted as they most likely reflect cells of endothelial and/or glial origin (Bayer and Altman, 1991).

Parvalbumin-positive neurons were detected using commercial primary antibodies (Sigma) on 25 or 30 μm floating cryosections. Total numbers of parvalbumin-positive neurons were determined by analyzing left and right hemispheres of four cerebral cortex sections at identical positions. All sections were processed identically to enable direct comparison.

Cardiovascular studies

Mean arterial blood pressure and heart rate were measured in awake, resting adult mice of 3–6 months of age. On the day of recording, mice were anesthetized with a single dose of intraperitoneal fentanyl (0.03 μg/g body weight), fluanisone (10 μg/g body weight) and midazolam (10 μg/g body weight). For blood pressure measurements, a polyethylene catheter (outer diameter: 400 μm) was inserted into the left carotid artery. If drugs were infused during the experimental protocol, a second polyethylene catheter of similar size was placed into the left jugular vein. All catheters were fixed to the vessel wall and led to the neck of the animal. Mice usually were awake <60 min after induction of anesthesia and were allowed to recover from surgical procedures for 5 h prior to recording baseline blood pressure. Each recording session lasted at least 10 min, and only episodes of physical rest were analyzed. During recordings, mice were placed in Plexiglas tubes to partially restrict their movements.

To induce chronic hypertension in female mice, angiotensin II (2 ng/g body weight/min) was infused continuously over 6 days using osmotic mini pumps (alzet, model 1007D). The osmotic pumps were implanted through a small neck incision during general anesthesia (see above). In a separate group of mice, a sham operation was performed. The dose of angiotensin II was adjusted to induce an increase in mean arterial blood pressure of ~20 mmHg in normal mice as determined in a series of pilot experiments. To minimize effects of confounding biological variables (initial body weight, age, genetic factors), female litter mates of the same genotype were assigned to both treatment groups in a paired fashion. On the day of recording, mice were given a carotid artery catheter during general anesthesia (see above), and blood pressure was measured as described above. Statistical comparisons between the different experimental groups were made using a two-way repeated measures analysis of variance (ANOVA) followed by the Bonferroni test for repeated comparisons.

Baroreflex control of blood pressure was studied in male mice using infusions of the β_1/β_2-adrenoceptor agonist isoproterenol. After baseline blood pressure was determined for at least 10 min, isoproterenol (0.05 ng/g body weight/min) was infused at a constant rate (0.25 μl/g body weight/ min) intravenously for 3 min. Blood pressure responses were averaged over the last 60 s of the infusion period. Then the infusion was stopped, and blood pressure was followed for another 3 min to assess the reversibility of the effects. To determine the critical isoproterenol dose, a dose–response curve was established as follows: six wild-type mice were infused with increasing doses of isoproterenol (0.05, 0.1 and 0.2 ng/g body weight/ min). This procedure was repeated twice and yielded the following results: 0.05 ng/g/min, –0.3 ± 1.7; 0.1 ng/g/min, –5.7 ± 7.1 mmHg; 0.2 ng/g/min, –22.7 ± 3.4 mmHg. Statistical comparisons were made between baseline and infusion periods using ANOVA (dose–response curve) or the paired Student's *t*-test. All animal experiments were approved by the local authorities and performed in accordance with the EMBL guidelines on animal experimentation.

Acknowledgements

The authors thank F.Casagranda and R.Klein for providing genomic libraries and ES cells for homologous recombination, G.Martin for providing the mouse FGF-2 cDNA, and A.Plück-Becklas, K.Brennan and M.Lemaistre of the EMBL TCF facility for generating mouse chimeras. We are indebted to K.Vintersten, J.Helppi, A.Reid and the EMBL animal technicians for excellent mouse care and help with animal procedures. We are grateful to G.Holländer and P.Monaghan for providing *in situ* probes, A.Neubüser for advice on non-radioactive section *in situ* hybridization, and J.Peters for performing the renin analysis. We are indebted to A.Haramis, A.Hohn, R.Klein, W.Kriz, F.Maina, L.Minichiello, D.Orioli, A.Postigo and H.Seller for helpful discussions during the analysis of the CNS phenotype. G.Davidson, F.Guillemot, A.Just and A.Zuniga are thanked for very helpful discussions and suggestions on the manuscript. This study was partially supported by an EU grant (CI1*CT93-0017) to R.Z.

References

Armstrong,R.C., Harvath,L. and Dubois-Dalcq,M. (1990) Type 1 astrocytes and oligodendrocyte-type-2 astrocyte glial progenitors migrate toward distinct molecules. *J. Neurosci. Res.*, **27**, 400–407.

Bannister,R. (1988) *Autonomic Failure—A Textbook of Clinical Disorders of the Autonomic Nervous System*. Oxford University Press, Oxford, UK.

Bayer,S.A. and Altman,J. (1991) *Neocortical Development*. Raven Press, Ltd, New York.

Celio,M.R. (1990) Calbindin D-28k and parvalbumin in the rat nervous system. *Neuroscience*, **35**, 375–475.

Chae,T., Kwon,Y.T., Bronson,R., Dikkes,P., Li,E. and Tsai,L.-H. (1997) Mice lacking p35, a neuronal specific activator of Cdk5, display cortical lamination defects, seizures and adult lethality. *Neuron*, **18**, 29–42.

Cheng,G.C., Briggs,W.H., Gerson,D.S., Libby,P., Grodzinsky,A.J., Gray,M.L. and Lee,R.T. (1997) Mechanical strain tightly controls fibroblast growth factor-2 release from cultured human vascular smooth muscle cells. *Circ. Res.*, **80**, 28–36.

Clarke,M.S.F., Caldwell,R.W., Chiao,H., Miyake,K. and McNeil,P.L. (1995) Contraction-induced cell wounding and release of fibroblast growth factor in heart. *Circ. Res.* **76**, 927–934.

Crossley,P.H., Martinez,S. and Martin,G.R. (1996) Midbrain development induced by FGF8 in the chick embryo. *Nature*, **380**, 66–68.

Cuevas,P., Carceller,F., Ortega,S., Zazo,M., Nieto,I. and Gimenez-Gallego,G. (1991) Hypotensive activity of fibroblast growth factor. *Science*, **254**, 1208–1210.

Cuevas,P. *et al*. (1996) Correction of hypertension by normalization of endothelial levels of fibroblast growth factor and nitric oxide synthase in spontaneously hypertensive rats. *Proc. Natl Acad. Sci. USA*, **93**, 11996–12001.

D'Arcangelo,G., Miao,G.G., Chen,S.C., Soares,H.D., Morgan,J.L. and Curran,T. (1995) A protein related to extracellular matrix proteins deleted in mouse mutant *reeler*. *Nature*, **374**, 719–723.

Davis,M.G., Zhou,M., Ali,S., Coffin,J.D., Doetschman,T. and Dorn,G.W. (1997) Intracrine and autocrine effects of basic fibroblast growth factor in vascular smooth muscle cells. *J. Mol. Cell. Cardiol*., **29**, 1061–1072.

D'Mello,S.R. (1998) Molecular regulation of neuronal apoptosis. *Curr. Top. Dev. Biol*., **39**, 187–213.

Dono,R. and Zeller,R. (1994) Cell-type-specific nuclear translocation of fibroblast growth factor-2 isoforms during chicken kidney and limb morphogenesis. *Dev. Biol*., **163**, 316–330.

Eckenstein,F.P. (1994) Fibroblast growth factors in the nervous system. *J. Neurobiol*., **25**, 1467–1480.

Fishell,G. and Hatten,M.E. (1991) Astrotactin provides a receptor system for CNS neuronal migration. *Development*, **113**, 755–765.

Ghosh,A. and Greenberg,M.E. (1995) Distinct roles for bFGF and NT-3 in the regulation of cortical neurogenesis. *Neuron*, **15**, 89–103.

Gisselbrecht,S., Skeath,J.B., Doe,C.Q. and Michelson,A.M. (1996) *heartless* encodes a fibroblast growth factor receptor (DFR1/DFGF-R2) involved in the directional migration of early mesodermal cells in the *Drosophila* embryo. *Genes Dev.*, **10**, 3003–3017.

Hatten,M.E. (1993) The role of migration in central nervous system neuronal development. *Curr. Opin. Neurobiol*., **3**, 38–44.

Hebert,J.M., Basilico,C., Goldfarb,M., Haub,O. and Martin,G.R. (1990) Isolation of cDNAs encoding four mouse FGF family members and characterization of their expression pattern during embryogenesis. *Dev. Biol*., **138**, 454–463.

Hebert,J.M., Rosenquist,T., Gotz,J. and Martin,G.R. (1994) FGF5 as a regulator of the hair growth cycle: evidence from targeted and spontaneous mutations. *Cell*, **78**, 1017–1025.

Howell,B.W., Hawkes,R., Soriano,P. and Cooper,J.A. (1997) Neuronal position in the developing brain is regulated by mouse disabled-1. *Nature*, **389**, 733–737.

Kardami,E. and Fandrich,R.R. (1989) Basic fibroblast growth factor in atria and ventricles of the vertebrate heart. *J. Cell Biol*., **109**, 1865–1875.

Kaye,D., Pimental,D., Prasad,S., Mäki,T., Berger,H.-J., McNeil,P.L., Smith,T.W. and Kelly,R.A. (1996) Role of transiently altered sarcolemmal membrane permeability and basic fibroblast growth factor release in the hypertrophic response of adult rat ventricular myocytes to increased mechanical activity *in vitro*. *J. Clin. Invest.*, **97**, 281–291.

Kim,S., Ohta,K., Hamaguchi,A., Yukimura,T., Miura,K. and Iwao,H. (1995) Angiotensin II induces cardiac phenotypic modulation and remodeling *in vivo* in rats. *Hypertension*, **25**, 1252–1259.

Kinoshita,Y., Kinoshita,C., Heuer,J.G. and Bothwell,M. (1993) Basic fibroblast growth factor promotes adhesive interactions of neuroepithelial cells from chick neural tube with extracellular matrix proteins in culture. *Development*, **119**, 943–956.

Klämbt,C., Glazer,L. and Shilo,B.Z. (1992) *breathless*, a *Drosophila* FGF receptor homologue, is essential for migration of tracheal and specific midline glial cells. *Genes Dev.*, **6**, 1668–1678.

Krege,J.H., John,S.W.M., Langenbach,L.L., Hodgkin,J.B., Hagaman, J.R., Bachman,E.S., Jennette,J.C., O'Brien,D.A. and Smithies,O. (1995) Male–female differences in fertility and blood pressure in ACE-deficient mice. *Nature*, **375**, 146–148.

Lazarous,D.F. *et al*. (1995) Effects of chronic systemic administration of basic fibroblast growth factor on collateral development in the canine heart. *Circulation*, **91**, 145–153.

Lee,S.M.K., Danielian,P.S., Fritzsch,B. and McMahon,A.P. (1997) Evidence that FGF8 signaling from the midbrain–hindbrain junction regulates growth and polarity in the developing midbrain. *Development*, **124**, 959–969.

Lindner,V. and Reidy,M.A. (1993) Expression of basic fibroblast growth factor and its receptor by smooth muscle cells and endothelium in injured rat arteries. *Circ. Res*., **73**, 589–595.

Mansour,S.L., Goddard,J.M. and Capecchi,M.R. (1993) Mice homozygous for a targeted disruption of the proto-oncogene *int-2* have developmental defects in the tail and inner ear. *Development*, **117**, 13–28.

Mathias,C.J. (1988) Cardiovascular control in spinal man. *Annu. Rev. Physiol*., **50**, 577–592.

Miller,K. and Rizzino,A. (1994) Developmental regulation and signal transduction of fibroblast growth factors and their receptors. In Wilson-Hamilton,M. (ed.), *Growth Factors and Signal Transduction in Development*. Wiley-Liss, Inc., New York, pp. 19–49.

Nagy,A., Rossant,J., Nagy,R., Abramow-Newerly,W. and Roder,J.C. (1993) Viable cell culture-derived mice from early passage embryonic stem cells. *Proc. Natl Acad. Sci. USA*, **90**, 8424–8428.

Neubuser,A., Peters,H., Balling,R. and Martin,G.R. (1997) Antagonistic interactions between FGF and BMP signaling pathways: a mechanism for positioning the site of tooth formation. *Cell*, **90**, 247–255.

Nurcombe,V., Ford,M.D., Wildchut,J.A. and Bartlett,P.F. (1993) Developmental regulation of neural response to FGF-1 and FGF-2 by heparan sulfate proteoglycan. *Science*, **260**, 103–106.

Ohshima,T., Ward,J.M., Huh,C.-G., Longenecker,G., Veeranna, Harish,C., Pant,H.C., Brady,R.O., Martin,L.J. and Kulkarni,A.B. (1996) Targeted disruption of the cyclin-dependent kinase 5 gene results in abnormal corticogenesis, neuronal pathology and perinatal death. *Proc. Natl Acad. Sci. USA*, **93**, 11173–11178.

Osterhout,D.J., Ebner,S., Xu,J., Ornitz,D.M., Zazanis,G.A. and McKinnon,R.D. (1997) Transplanted oligodendrocyte progenitor cells expressing a dominant-negative FGF receptor transgene fail to migrate *in vivo*. *J. Neurosci*., **17**, 9122–9132.

Petroski,R.E., Grierson,J.P., Choi-Kwon,S. and Geller,H.M. (1991) Basic fibroblast growth factor regulates the ability of astrocytes to support hypothalamic neuronal survival *in vitro*. *Dev. Biol*., **147**, 1–13.

Qian,X., Davis,A.A., Goderie,S.K. and Temple,S. (1997) FGF2 concentration regulates the generation of neurons and glia from multipotent cortical stem cells. *Neuron*, **18**, 81–93.

Ray,J., Peterson,D.A., Schinstine,M. and Gage,F.H. (1993) Proliferation, differentiation and long-term culture of primary hippocampal neurons. *Proc. Natl Acad. Sci. USA*, **90**, 3602–3606.

Riese,J., Zeller,R. and Dono,R. (1995) Nucleo-cytoplasmic translocation and secretion of fibroblast growth factor-2 during avian gastrulation. *Mech. Dev*., **49**, 13–22.

Sasai,Y. and De Robertis,E.M. (1997) Ectodermal patterning in vertebrate embryos. *Dev. Biol*., **182**, 5–20.

Soriano,E., Alvarado-Mallart,R.M., Dumesnil,N., Del Rio,J.A. and Sotelo,C. (1997) Cajal–Retzius cells regulate the radial glia phenotype in the adult and developing cerebellum and alter granule cell migration. *Neuron*, **18**, 563–577.

Stapf,C., Lück,G., Shakibaei,M. and Blottner,D. (1997) Fibroblast growth factor-2 (FGF-2) and FGF-receptor (FGFR-1) immunoreactivity in embryonic autonomic neurons. *Cell Tissue Res*., **287**, 471–480.

Sutherland,D., Samakovlis,C. and Krasnow,M.A. (1996) *branchless* encodes a *Drosophila* FGF homologue that controls tracheal cell migration and the pattern of branching. *Cell*, **87**, 1091–1101.

Temple,S. and Qian,X. (1995) bFGF, neurotrophins and the control of cortical neurogenesis. *Neuron*, **15**, 249–252.

Tybulewicz,V.L.J., Crawford,C.E., Jackson,P.K., Bronson,R.T. and Mulligan,R.C. (1991) Neonatal lethality and lymphopenia in mice with a homozygous disruption of the c-abl proto-oncogene. *Cell*, **65**, 1153–1163.

Vescovi,A.L., Reynolds,B.A., Fraser,D.D. and Weiss,S. (1993) bFGF regulates the proliferative fate of unipotent (neuronal) and bipotent (neuronal/dstroglial) EGF-generated CNS progenitor cells. *Neuron*, **11**, 951–966.

Vicario-Abejon,C., Johe,K.K., Hazel,T.G., Collazo,D. and McKay,R.D. (1995) Function of basic fibroblast growth factor and neurotrophins in the differentiation of hippocampal neurons. *Neuron*, **15**, 105–114.

Wilcox,B.J. and Unnerstall,J.R. (1991) Expression of acidic fibroblast growth factor mRNA in the developing and adult rat brain. *Neuron*, **6**, 397–409.

Wilkinson,D.G., Peters,G., Dickson,C. and McMahon,A.P. (1988) Expression of the FGF-related proto-oncogene *int-2* during gastrulation and neurulation in the mouse. *EMBO J*., **7**, 691–695.

Wurst,W. and Joyner,A.L. (1993) Production of targeted embryonic stem cell clones. In Joyner,A.L. (ed.), *Gene Targeting: A Practical Approach*. IRL Press, Oxford, UK, pp. 33–61.

Yamaguchi,T.P., Harpal,K., Henkemeyer,M. and Rossant,J. (1994) fgfr-1 is required for embryonic growth and mesodermal patterning during mouse gastrulation. *Genes Dev.*, **8**, 3032–3044.

Yayon,A., Ma,Y., Safran,M., Klagsbrun,M. and Halaban,R. (1997) Suppression of autocrine cell proliferation and tumorigenesis of human melanoma cells and fibroblast growth factor transformed fibroblasts by a kinase-deficient FGF receptor 1: evidence for the involvement of Src-family kinases. *Oncogene*, **14**, 2999–3009.

Zhan,X., Plourde,C., Hu,X., Friesel,R. and Maciag,T. (1994) Association of fibroblast growth factor receptor-1 with c-Src correlates with association between c-Src and cortactin. *J. Biol. Chem.*, **269**, 20221–20224.

Zhou,M. *et al*. (1998) Fibroblast growth factor 2 control of vascular tone. *Nature Med.*, **4**, 201–207.

Zuniga Mejia Borja,A., Murphy,C. and Zeller,R. (1996) *alt*FGF-2, a novel ER-associated FGF-2 protein isoform: its embryonic distribution and functional analysis during neural tube development. *Dev. Biol.*, **180**, 680–692.

Received April 22, 1998; revised and accepted June 4, 1998